

# Diphoton Trigger Efficiency Study in $3\text{ fb}^{-1}$ of CDF II data

Mirco Dorigo<sup>1</sup>, Shin-Shan Eiko Yu<sup>2</sup>

October 1, 2008

<sup>1</sup>*Department of Physics, University of Trieste, Italy*

<sup>2</sup>*Fermi National Accelerator Laboratory, Batavia, IL*

## Abstract

A study of the diphoton trigger efficiency in  $p\bar{p}$  collisions at  $\sqrt{s} = 1.96\text{ TeV}$  using the CDF II detector is presented. The target is to update the diphoton trigger efficiency measurement dated August 2004 [1], using  $3\text{ fb}^{-1}$  of data. The transverse energy selection efficiency for the central diphoton trigger is measured. Also a study on the plug photon is contained. Finally, a note is reported on how the efficiency depends on the EM calorimeter isolation cut.

# 1 Introduction

This is a study of the diphoton trigger efficiency in  $p\bar{p}$  collisions at  $\sqrt{s} = 1.96\text{ TeV}$  using the CDF II detector. It is very important to measure the diphoton trigger efficiency because it can be involved in different kinds of researches (both in Standard Model and beyond) which use photons in their analysis. Here is a list of them:

- $\gamma\gamma$  cross-section;
- Signature-based search, in which the final state is  $\gamma\gamma + X$ , where  $X$  can be missing energy, leptons, jets or  $\gamma$ ;
- The  $H \rightarrow \gamma\gamma$  decay mode, that is a useful channel for the SM Higgs boson and fermiophobic Higgs searches in the low mass region ( $M_H < 130\text{ GeV}$ );
- Fermiophobic Higgs, with the  $H^+h \rightarrow W^+hh \rightarrow W^+ + 4\gamma$  decay mode;
- Randall-Sundrum Graviton, with the  $G_{RS} \rightarrow \gamma\gamma$  decay mode;

An update of diphoton trigger efficiency is required for two reasons. First, the last measurement of the diphoton trigger efficiency that can be used at the moment is found in [1]. This is dated August 2004, about four years ago. Second, in October 2007 the level 2 trigger has been upgraded.

Besides, in hadronic collider, photon signals are contaminated by the production of neutral mesons which decay to multiple collinear photons. The experience of understanding the background contamination in the trigger efficiency with Tevatron data is very important also for the forthcoming LHC experiments.

The scheme of the presentation is as follows. Sections 2 describes the differences between the offline and online reconstruction. Section 3 is about the definition of the diphoton trigger efficiency and some explanations on how it is measured. The diphoton cuts and the data used in the analysis are presented in Section 4. Section 5 is divided in two subsections: in the first one is the measurement of the transverse energy selection efficiency of diphoton trigger for central photons; the second one reports a study for plug photon. Section 6 concerns about the introduction of calorimeter isolation cut at the trigger level. Section 7 is for the conclusions.

## 2 The reconstruction of the events

There are two kinds of reconstruction of the events: online and offline. The online reconstruction is made by the trigger. The CDF detector<sup>1</sup> has 3 trigger levels. The trigger decisions on the events selection have to be very quick, so the algorithms involved are simple as efficient as possible. Instead, in the offline reconstruction there is enough time to add more informations for advanced algorithmes and calibration. The result is that there are two different versions of reconstruction, resulting in slightly different EM quantities. For example, photon variables were calculated assuming  $z_{\text{Vertex}} = 0$  at Level 2 (L2) and Level 3 (L3), causing smearing between online and offline transverse energy ( $E_t$ ) (See Fig. 1). The difference between online and offline might have introduce some inefficiency to trigger. L2 uses different clustering algorithm, and isolation definition, which might have caused some more inefficiency.

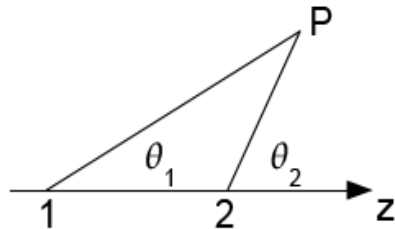


Figure 1:  $E_t$  is different if the  $z_{\text{Vertex}}$  is the point 1 or the point 2. In this case  $E_{t1} = E \sin \theta_1 < E_{t2} = E \sin \theta_2$

## 3 The diphoton Trigger efficiency

See Fig. 2. “A” is the set of events from inclusive photon trigger (PHOTON\_25\_ISO) with the requirements to have two offline photons. “B” is the set of events selected by the diphoton trigger. So, in general, the definition of the *diphoton trigger efficiency per leg* is the ratio of these two events

$$Eff = \frac{B}{A} \quad (1)$$

---

<sup>1</sup>The CDF detector is described in many available references [2, 3, 4]

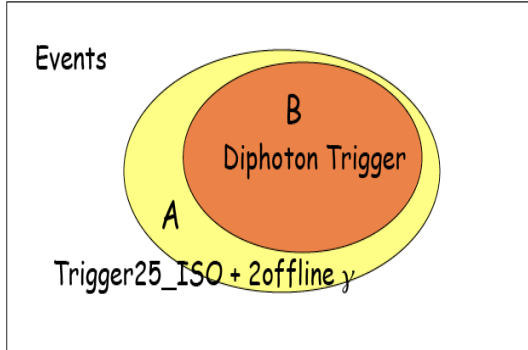


Figure 2: A schematic representation of the sets of events used to evaluate the diphoton trigger efficiency.

The definition is called *per leg*: this means that photon pass diphoton trigger one by one. We assume that the two photons are not correlated, so the total efficiency is the product of the efficiency for the two legs. For each event that passes the inclusive single photon trigger (*A*), we count how often the next-to-leading photon passes the cuts of the diphoton trigger (*B*). The next-to-leading photon is the second highest energy photon. This can be interpreted as the probability of the next-to-leading photon leg satisfying the diphoton trigger requirement.

In this study, events from inclusive photon trigger (PHOTON\_25\_ISO) are used for the denominator of the previous definition 1. The numerator needs a particular explanation: it is the matching between the next-to-leading offline photon and trigger (for L2 TPhotonUtil::L2ClusterMatch). This because the first intention is to measure only the transverse energy selection efficiency for diphoton trigger.

## 4 Diphoton Cuts and data used

The table 1 lists the diphoton trigger cuts. This study focuses on L2 and L3. Level 1 trigger efficiency has been found to be fully efficient in Ref. [6].

Samples from February 2002 (sam 0d) to April 2008 (sam 0k) are used, which correspond to an integrated luminosity of  $3 fb^{-1}$ . The measurement is made for samples from 0d to 0j together. In order to compare the efficiencies before and after the L2 trigger upgrade (October 2007), sample 0k is separated from the others.

Level 1
single trigger tower $E_t > 8 \text{ GeV}$ HadEm< 0.125 [4, 5]
Level 2
Two high em pass Em Clusters (clustering with trigger-tower-segmentation [5])
HadEm< 0.125
Isolation< 3 GeV .or. Isofraction< 0.15
$E_t > 10 \text{ GeV}$
Level 3
Two em objects
average CES $\chi^2 < 20$
$E_t > 12 \text{ GeV}$
HadEm< $0.055 + 0.00045 * E_t$
Isolation< 2 GeV .or. isofraction< 0.1

Table 1: Diphoton trigger specification. Note that L2 and L3 quantities are formed with  $z_{\text{Vertex}} = 0$ .

## 5 Transverse energy selection trigger efficiency

As mentioned above, first of all the energy selection efficiency for diphoton trigger is focused: all cuts are removed, except the one on energy.

### 5.1 Central photons

Let start looking at the distributions of numerator and denominator of the efficiency for samples from 0d to 0j together. They are shown in Fig. 3.

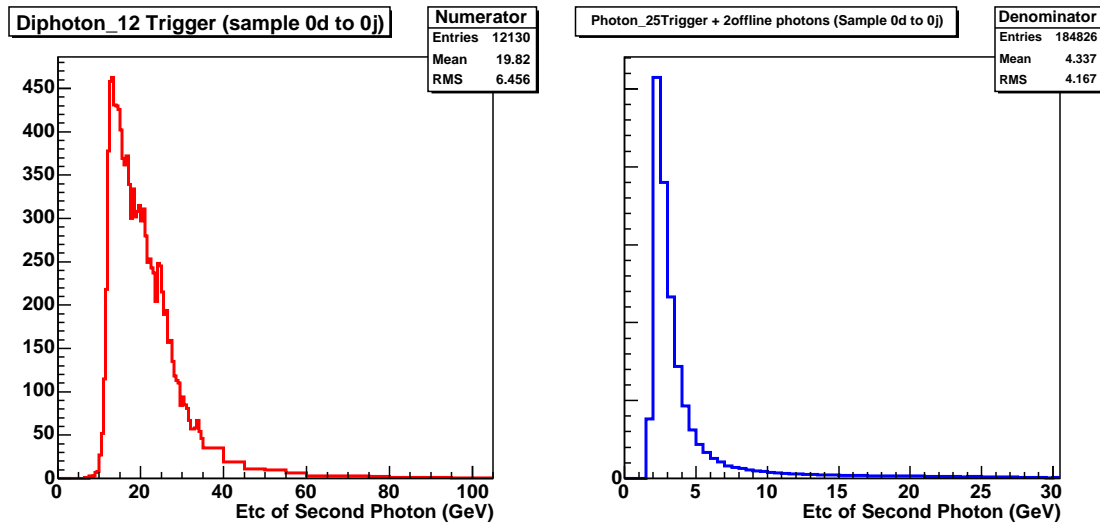


Figure 3: Sample from 0d to 0j merged together for central photons. On the left the plot of the next-to-leading photon correct transverse energy ( $E_{\text{tc}}$ ) distribution for numerator; on the right the same for denominator.

The resulting efficiency is plotted in Fig. 4.

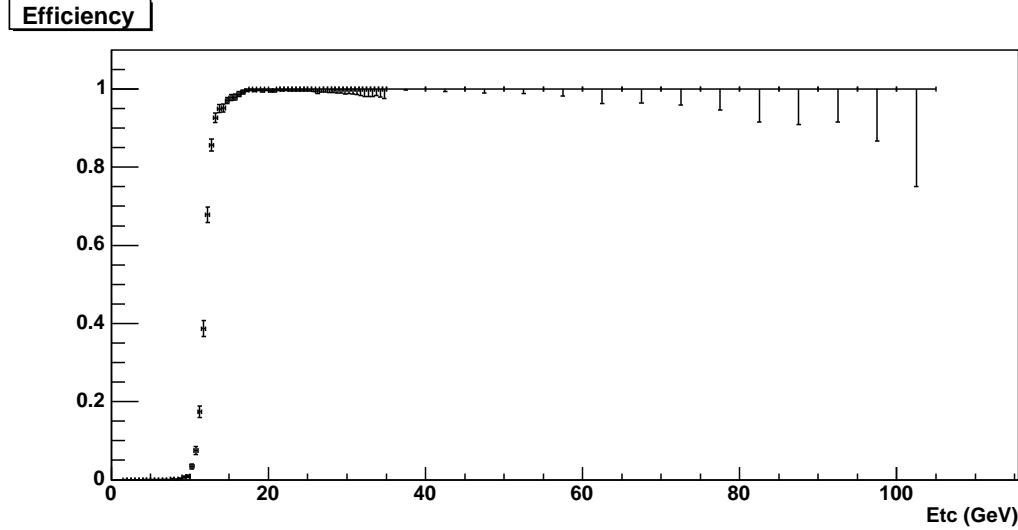


Figure 4: Energy selection trigger efficiency versus  $E_{\text{tc}}$  for samples from 0d to 0j merged together (all the computed efficiency uncertainties are asymmetric bayesian errors).

The same three plots for the sample 0k are in Fig. 5 and Fig. 6.

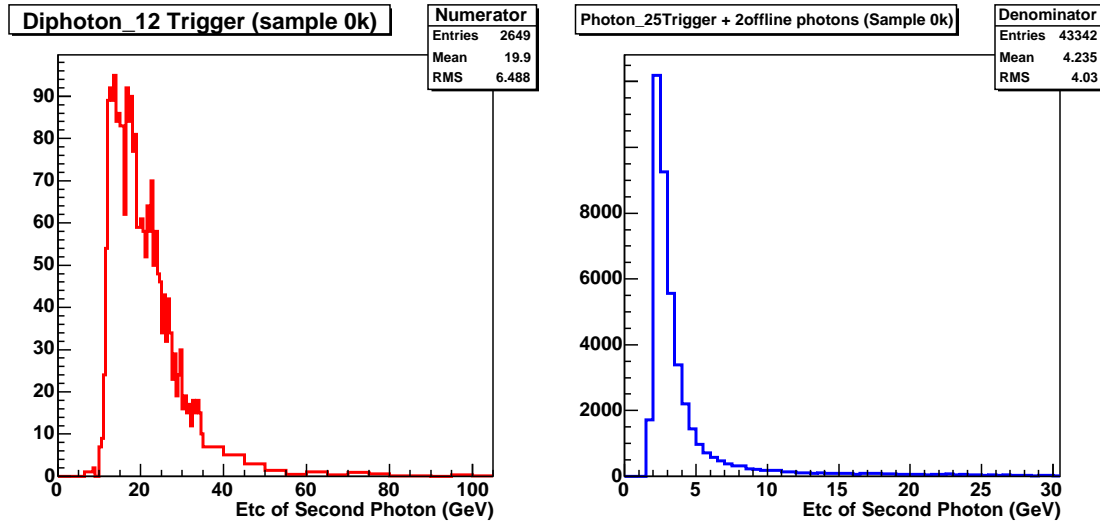


Figure 5: Sample 0k for central photons. On the left the plot of the next-to-leading photon  $E_{\text{tc}}$  distribution for numerator; on the right the same for denominator.

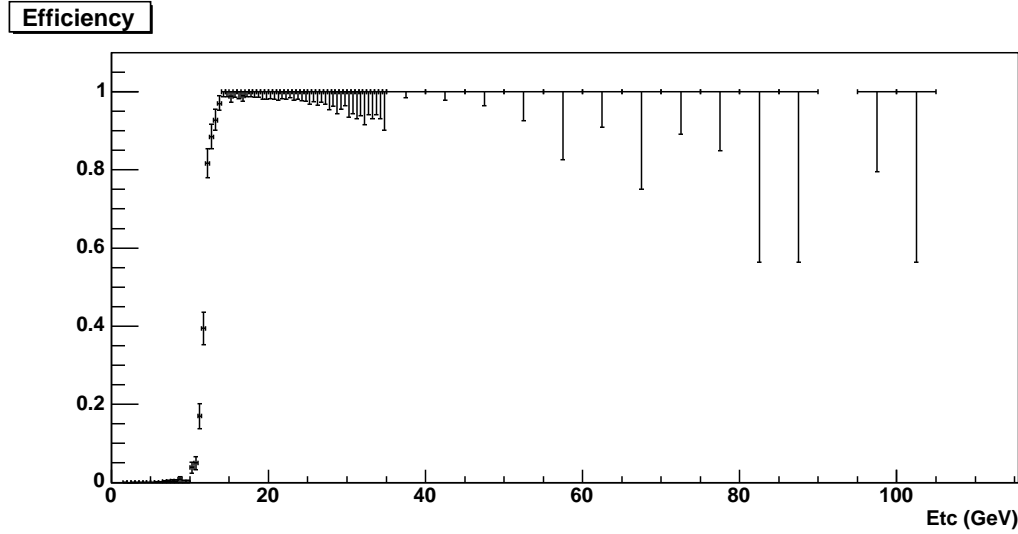


Figure 6: Energy selection trigger efficiency versus  $E_{\text{tc}}$  for samples 0k (all the computed efficiency uncertainties are asymmetric bayesian errors).

The Efficiency can be parameterized as

$$p0 * \text{Erfc}(p1 * (p2 - Etc)) \quad (2)$$

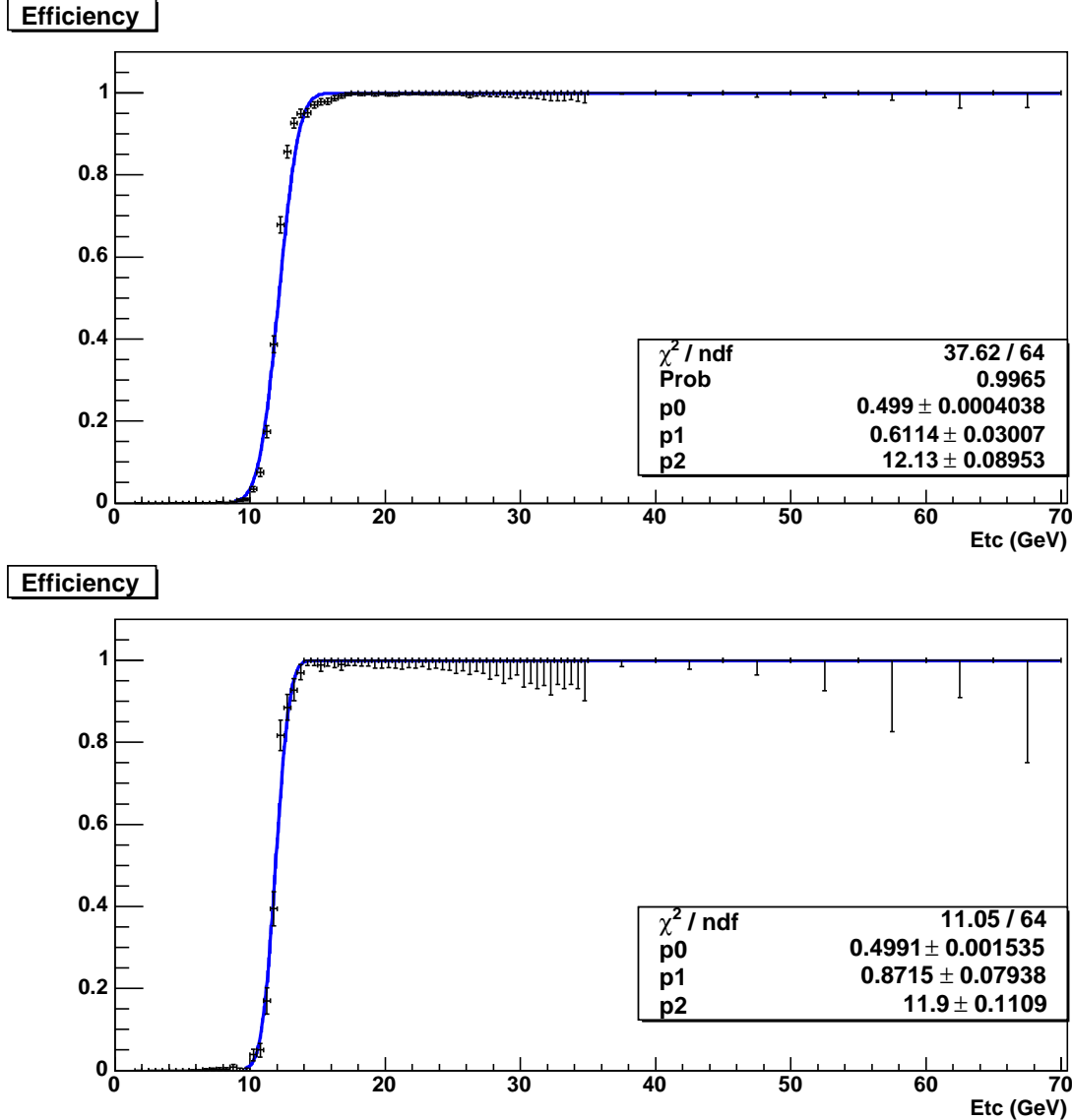


Figure 7: Fit of the efficiency (all the computed efficiency uncertainties are asymmetric bayesian errors). Above: samples from 0d to 0j together. Under: sample 0k.

As one can see in the Fig. 7, the parameter  $p1$ , that is related to the turning on of

the fitting function, is greater for sample 0k than for the others. So it seems that the transverse energy selection diphoton efficiency is better after the L2 upgrade.

	sample 0d-0j	sample 0k
$p1$	$0.61 \pm 0.03$	$0.87 \pm 0.08$

This also confirmed by the overlapping of the two plot: the efficiency for sample 0k reaches 1 before the one of the other samples (Fig. 8).

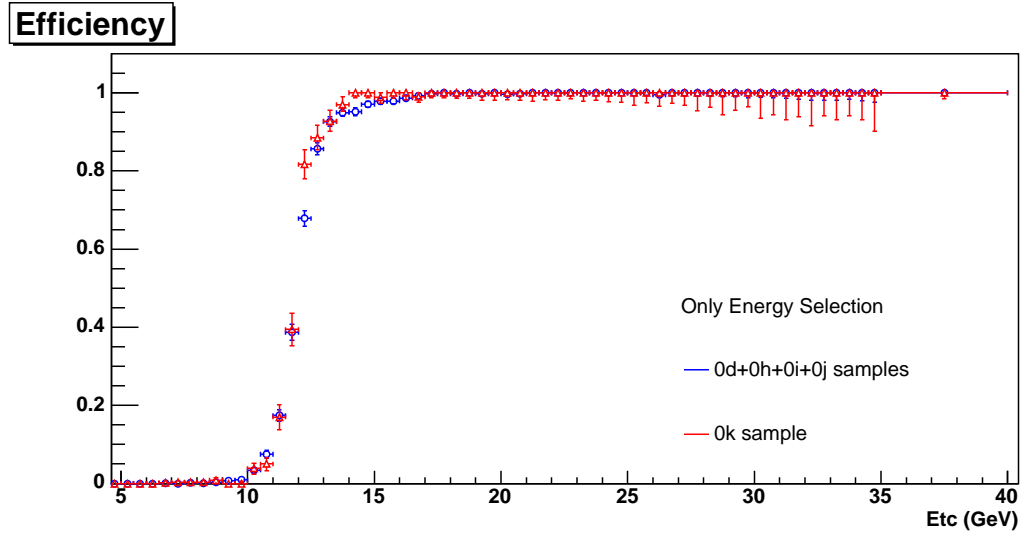


Figure 8: Overlap of the two previous efficiency plots. The sample 0k (red points) turn on and reach 1 faster than the others samples (blue points).

The following figure (Fig. 9) is the overlap of the plot of the efficiency for every sample separately drawn.

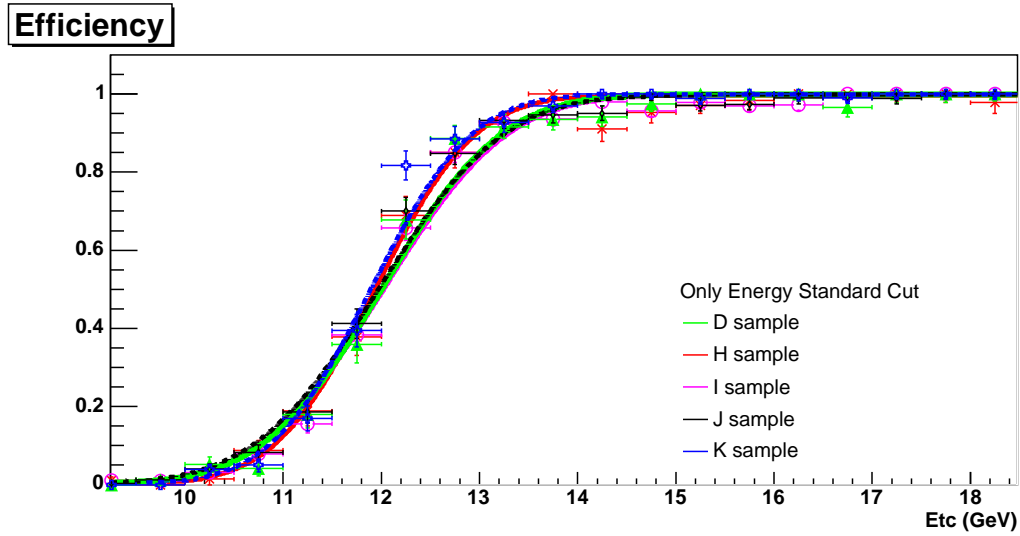


Figure 9: Overlap of the efficiency plots for every sample.

## 5.2 Plug photons

To introduce the plug photons in the analysis, the code used to fill the histograms of numerator and denominator is changed in this points:

- the leading photon can be both central and plug;
- the case of central next-to-leading photon is separated from the plug one.

The result is that the plot of efficiency versus the next-to-leading  $E_{tc}$  for the central photons is similar to that is showed before (see Fig. 10 and compare with Fig. 7).

Instead, when the next-to-leading is a plug photon, the efficiency dramatically changes and it is never greater than 90% when the  $E_{tc}$  is less than 80  $GeV$ . This can be seen in Fig. 11.

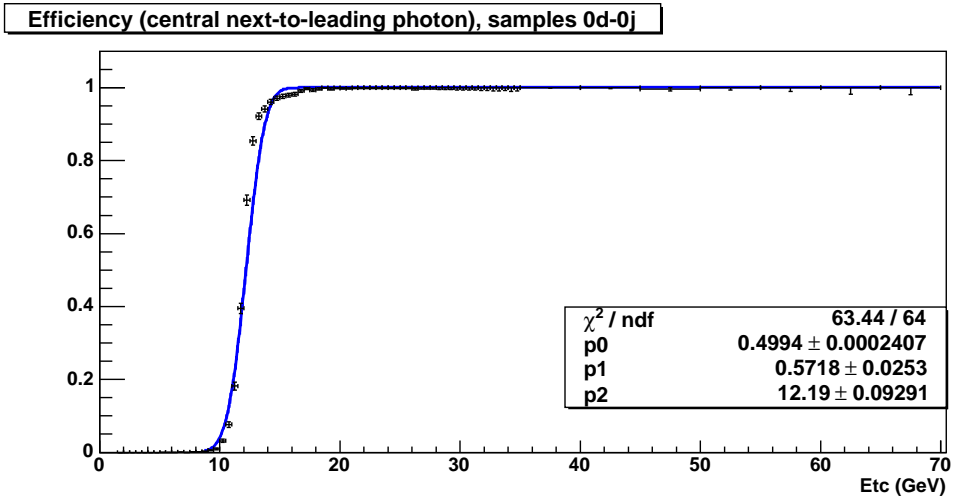


Figure 10: Plot of efficiency versus  $E_{\text{tc}}$  (all the computed efficiency uncertainties are asymmetric bayesian errors). The leading photon can be both central or plug. The next-to-leading is central photon. Note that the error bars is less than the same plot in Fig. 7 where the leading photon is only central. In fact, here there are more statistics (this is confirmed by the better  $\chi^2/\text{ndf}$ ; on the other hand the parameter  $p1 = 0.57 \pm 0.02$  is less than the previous one).

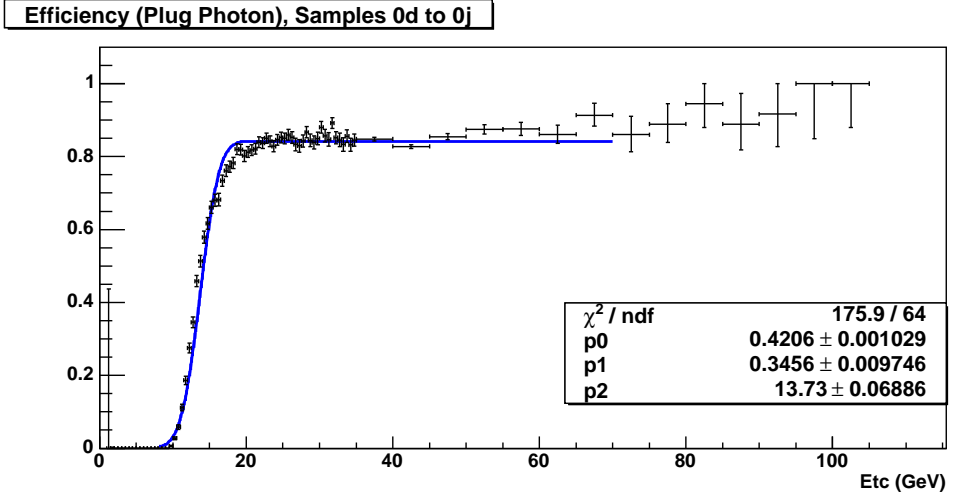


Figure 11: Plot of efficiency versus  $E_{\text{tc}}$  (all the computed efficiency uncertainties are asymmetric bayesian errors). The leading photon can be both central or plug. The next-to-leading is plug photon.

The reason of this behaviour have to be searched in the L2 seed tower. In fact, it is found that the L2 seed tower could be incorrect by  $\pm 1$  trigger tower about 20% of the time. L2 cluster match in `TPhotonUtil::L2ClusterMatch` requires  $\Delta R$  between offline and trigger  $< 0.4$  (remind that  $\Delta R = \sqrt{(\Delta\eta)^2 + (\Delta\phi)^2}$ ). For trigger tower with  $|\eta| > 1.6$  plug photon fails matching more easily than central photon because the trigger tower size increases from  $\Delta\eta = 0.2$  to  $\Delta\eta = 0.3, 0.4$  and  $0.7$ . Removing the requirement on  $\Delta R$ , the efficiency improves, but it doesn't reach the level of goodness of that for the central photons yet. This is showed in Fig. 12.

The efficiency for the central photons is still best in comparison to plug photons (see Fig. 13) because of the calculation online of the  $E_t$  assuming the  $z_{\text{Vertex}} = 0$ . In fact, the plug photons are more sensitive to the difference between online and offline reconstruction mentioned in Section 2 (see also Fig. 1). This can be seen in Fig. 15 where the efficiency is plot with the offline requirement that  $|z_{\text{Vertex}}| < 5 \text{ cm}$  (red points) and  $|z_{\text{Vertex}}| > 30 \text{ cm}$ . When the  $E_t$  from online is not closer to the one offline (blue points), the efficiency turns on later.

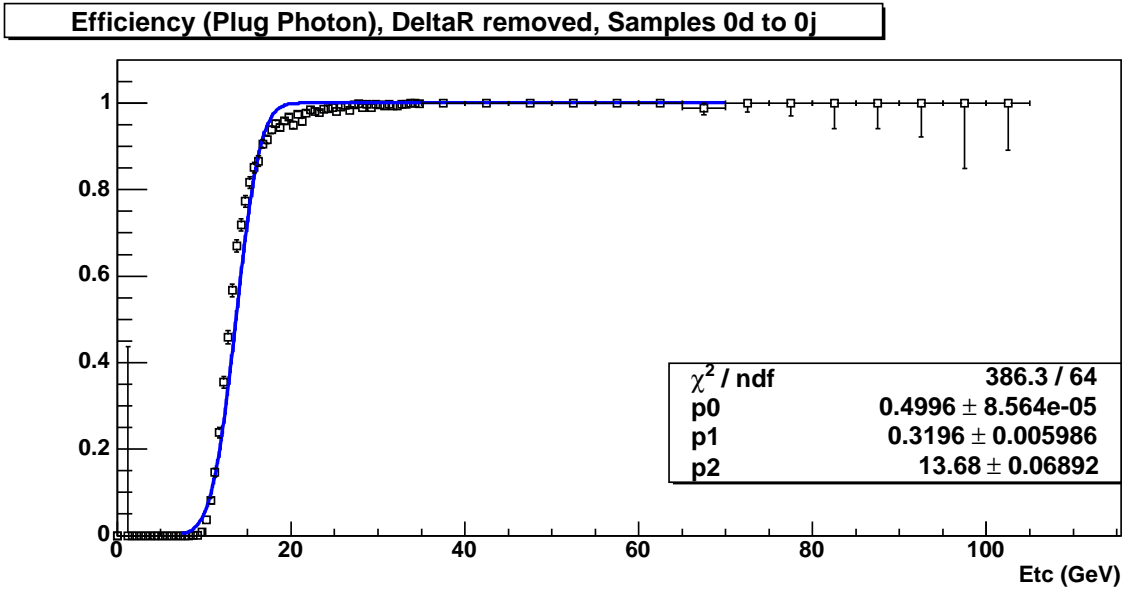


Figure 12: Plot of efficiency versus  $E_{\text{tc}}$  with  $\Delta R$  cut removed (all the computed efficiency uncertainties are asymmetric bayesian errors). The leading photon can be both central or plug. The next-to-leading is plug photon.

Efficiency DeltaR removed, Samples 0d to 0j

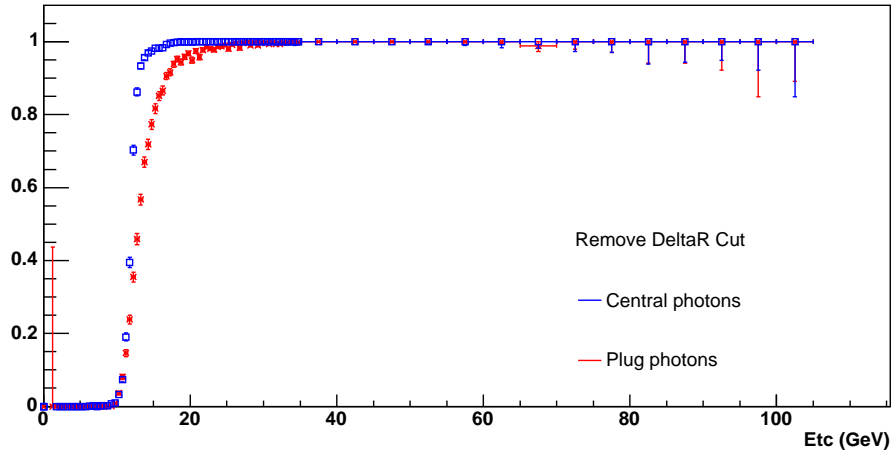


Figure 13: Overlap of the plot of efficiency for the central photons of Fig. 10 and the plot of efficiency for the plug photons with  $\Delta R$  cut removed (Fig. 12).

Efficiency

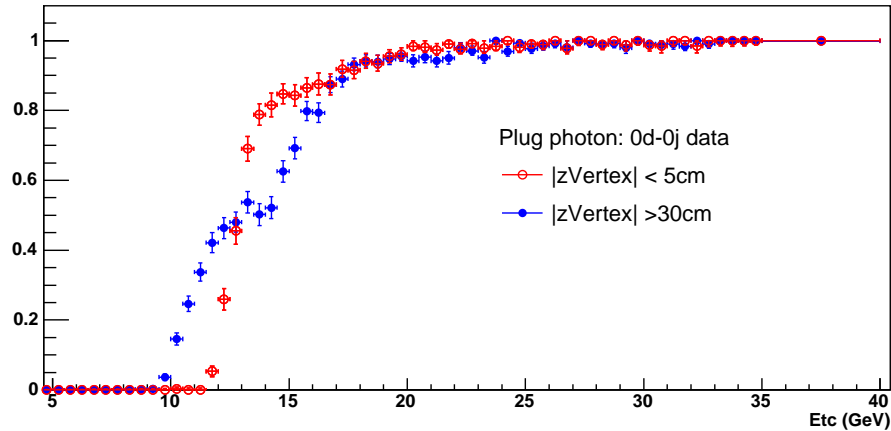


Figure 14: Plot of efficiency versus  $E_{tc}$  for samples from 0d to 0j together without the  $\Delta R$  cut as before (all the computed efficiency uncertainties are asymmetric bayesian errors). The red point are related to the offline requirement that  $|z_{\text{Vertex}}| < 5\text{ cm}$ ; the blue points are for  $|z_{\text{Vertex}}| > 30\text{ cm}$ . Note that when offline  $z_{\text{Vertex}}$  is closer to the online one the efficiency is better (remind online always has  $z_{\text{Vertex}} = 0$ ).

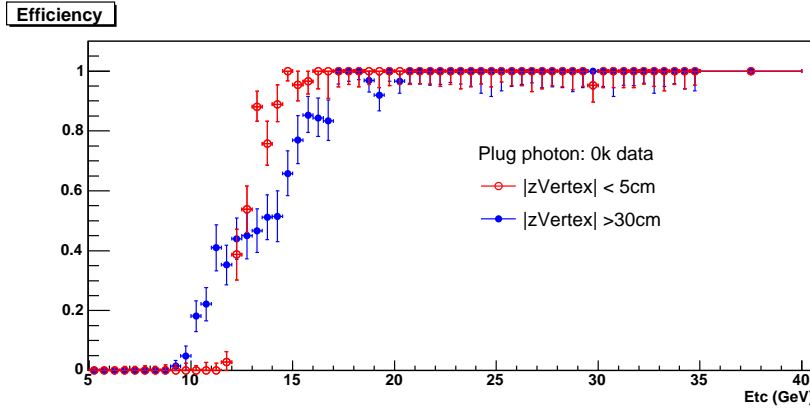


Figure 15: Plot of efficiency versus  $E_{tc}$  for sample 0k without the  $\Delta R$  cut as before (all the computed efficiency uncertainties are asymmetric bayesian errors). The red point are related to the offline requirement that  $|z_{\text{Vertex}}| < 5 \text{ cm}$ ; the blue points are for  $|z_{\text{Vertex}}| > 30 \text{ cm}$ . Note that when offline  $z_{\text{Vertex}}$  is closer to the online one the efficiency is better (remind online always has  $z_{\text{Vertex}} = 0$ ).

## 6 Calorimeter Isolation Cut

If we introduce also the calorimeter isolation cut in Table 1 to our trigger requirements, starting from the standard offline cut (see Appendix A), the result is showed in Fig. 16.

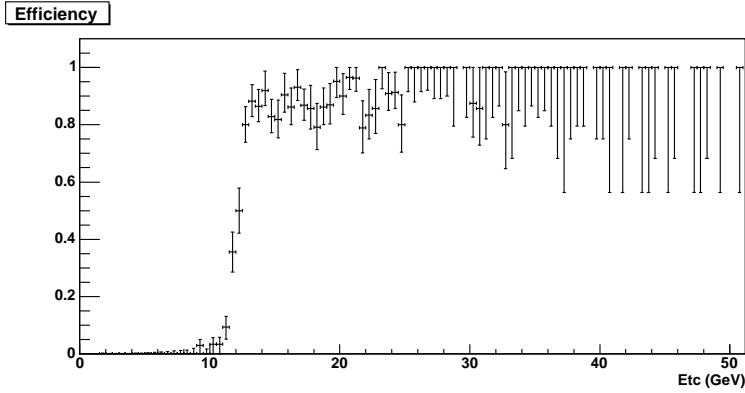


Figure 16: Efficiency versus  $E_{tc}$  for sample 0k (all the computed efficiency uncertainties are asymmetric bayesian errors). In this plot the calorimeter isolation cut is introduced at the L2 and L3 trigger tracking requirements.

This because the ratio signal/background depend on energy and in the low energy region there is more contamination of background. The isolation is very sensitive to the background. This can be seen introducing a tighter cut in the offline (instaed of the isolation cuts in Appendix A, isolation cut at  $1\text{ GeV}$  is applied). In fact, taking offline isolation in  $0.4$  cone  $< 1\text{ GeV}$ , the background contamination is removed and the efficiency changes as it showed in Fig. 17. The choice of a tighter offline cut is adopted in [1].

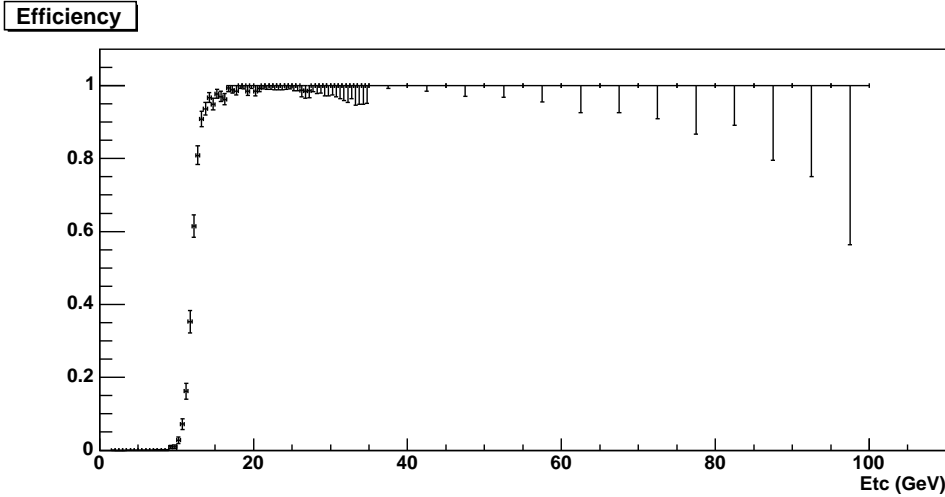


Figure 17: Efficiency versus  $E_{\text{tc}}$  (all the computed efficiency uncertainties are asymmetric bayesian errors) with a tighter cut on calorimeter isolation in the offline (Iso in  $0.4$  cone  $< 1\text{ GeV}$ )

So samples with less background have to be used: this is the case of electrons samples. Indeed, electron samples have more pure signal and the trigger for electrons and photons shower is exactly the same, since the track identification is not involved.

## 7 Conclusion

The complete measurement done in this documentation is the central and plug diphoton trigger efficiency for energy selection before and after the L2 trigger upgrade in  $3\text{ fb}^{-1}$  of CDF II data. It can be concluded that the diphoton trigger efficiency reaches 100% at  $E_{\text{tc}} = 17\text{ GeV}$  for the central photons and at  $E_{\text{tc}} = 25\text{ GeV}$  for plug photons (see Fig. 13). In order to completely update the measurement in [1], the efficiency introducing all trigger cuts (not only the energy one) has to be studied, similar to what is done here

for the calorimeter isolation. Besides, to reach this target, the adoption of more pure samples (like the electrons samples) is advisable.

## Appendix A: Standard offline Cuts

Variable	Standard Cut
Correct Et	$> 7 \text{ GeV}$ or more
CES X and Z Fiducial	$\text{Ces }  X  < 21 \text{ cm}, 9 < \text{Ces }  Z  < 230 \text{ cm}$
Had/Em	$< 0.055 + 0.00045 * \text{Ecorr}$
Cone 0.4 IsoEtc	$Etc < 20 \text{ GeV}: < 0.1 * Etc; Etc > 20 \text{ GeV}: < 2.0 + 0.02 * (Etc - 20)$
Chi2 (Strips+Wires)/2	$< 20$
N track (N3D)	$\leq 1$
Track Pt	$< 1 + 0.005 * Etc \text{ GeV}$
Cone 0.4 Track Iso	$< 2 + 0.005 * Etc \text{ GeV}$
2 <sup>nd</sup> CES cluster $E * \sin\theta$	$Etc < 18 \text{ GeV}: < 0.14 * Etc; Etc > 18 \text{ GeV}: < 2.4 + 0.01 * (Etc - 20)$

Table 2: Standard offline cuts for central photons (see also the photon instructions web page <http://www-cdf.fnal.gov/internal/physics/photon/docs/cuts.html>)

Variable	Standard Cut
PES U and V Fiducial	$1.2 < Eta \text{ det} < 2.8$
Had/Em	$\text{ECorr} < 100 \text{ GeV}: < 0.5; \text{ECorr} > 100 \text{ GeV}: < 0.05 + 0.026 * \ln(\text{ECorr}/100)$
Cone 0.4 IsoEtc	$Etc < 20 \text{ GeV}: < 0.1 * Etc; Etc > 20 \text{ GeV}: < 2.0 + 0.02 * (Etc - 20)$
PEM Chi2	$< 10$
PES 5/9	$> 0.65$
Cone 0.4 Track Iso	$< 2 + 0.005 * Etc \text{ GeV}$

Table 3: Standard offline cuts for plug photons (see also the photon instructions web page <http://www-cdf.fnal.gov/internal/physics/photon/docs/plugcuts.html>)

## References

[1] CDF Note 6312 *Isolated prompt diphoton central-central cross-section measurement at CDF Run II*, Robert Blair, Raymond Culberston, Joey Huston, Steve Kuhlmann, Yanwen Liu, Xin Wu.

- [2] F. Abe et al. (CDF), Nucl. Instr. Meth **A271**, 387 (1988).
- [3] P. T. Lukens (CDF IIb) (2003), FERMILAB-TM-2198.
- [4] FERMILAB-Pub-96/390-E *The CDF II Detector Technical Design Report* Chap 12, the CDF II collaboration.
- [5] CDF Note 2045 *Trigger tower organization and summing in  $\eta - \phi$  space for Run II and beyond.* H. J. Frisch, M. Shochet, G. Sullivan, P. J. Wilson.
- [6] CDF/DOC/ELECTRON/CDFR/6234 *Trigger Efficiencies for High  $P_T$  Electrons,* Young-Kee Kim, Jason Nielsen, Lauren Tompkins, Greg Veramendi.